Interactions and Conformations of α-Helical Human Apolipoprotein CI on Hydrophilic and on Hydrophobic Substrates

José Campos-Terán*

Instituto de Física, UNAM, P.O. Box 20-364, México D. F. 01000

Jaime Mas-Oliva

Instituto de Fisiología Celular, UNAM, P.O. Box 70-243, México D. F. 04510

Rolando Castillo

Instituto de Física, UNAM, P.O. Box 20-364, México D. F. 01000

Received: April 19, 2004; In Final Form: June 18, 2004

Interactions between amphiphilic α-helical human apolipoprotein CI (APO CI) adsorbed on hydrophilic and on hydrophobic surfaces were studied using an interferometric surface force apparatus in an effort to understand the surface conformation and the binding activity of this protein. We used mica as the hydrophilic substrate and polymerized octadecyltriethoxysilane (OTE)-covered mica as the hydrophobic substrate. The OTE monolayer and the OTE Langmuir–Blodgett film were studied using Brewster angle microscopy and atomic force microscopy, respectively. We found that interaction forces between layers of APO CI adsorbed on hydrophilic and on hydrophobic surfaces are mainly due to electrostatic double-layer forces at large surface distances and to steric repulsive forces at small distances. In some cases, no force was measured prior to finding a steric wall, suggesting that a complete neutralization of the surface charge was achieved by the protein adsorption. Protein layer thickness values allow us to give an image of the organization and conformation of the APO CI protein on surfaces. The adhesion obtained in both kinds of surfaces indicates that the interaction between the hydrophobic sides of the APO CI proteins is stronger than that between the hydrophilic sides of the protein.

Introduction

Apolipoprotein (APO) CI is composed of 57 amino acid residues, with a molecular mass of 6.63 kDa. Secondary structure predictions, nuclear magnetic resonance, and circular dichroism studies with APO CI have revealed a high α-helix content, distributed in two α-helices.[1-3] The first α-helix (residues 4–30) presents approximately 7.5 periods, while the second one (residues 35–53) consists of 5.2 periods. This protein forms part of a family of protein constituents of the high-density lipoproteins which are related to reverse cholesterol transport.[4] Apolipoproteins are membrane active proteins with amphiphilic character, since a polar protein face is formed by charged amino acid residues clustered on one side of the α-helices, whereas a hydrophobic surface composed of nonpolar residues is formed at the opposite face of the α-helices.[1-3,5] When these proteins are in contact with a polar or nonpolar medium, their natural tendency is to anchor the hydrophilic and hydrophobic regions in the polar and nonpolar media, respectively. Thus, a hydrophobic–hydrophilic interface tends to induce a specific orientation on the adsorbed molecules.

Models of lipoprotein particles[6] are basically spheres made of a phospholipid monolayer filled up with triglycerides and cholesterol esters, where the phospholipid heads are in contact with the plasma. In these models, APOs are usually placed lying down on the lipoprotein particles.[1,6] A way to understand the behavior of APOs on the lipoprotein surface is to deposit them on an interface that models the lipoprotein surface, which could be increasingly complex as needed. The first attempts in this direction have used APO CI Langmuir monolayers deposited at the air–water interface.[2,3] Here, the monolayer exhibited two first-order phase transitions. One of them ($\Pi \sim 33$ mN/m and $A \sim 350-600$ Å^2/molecule) that could have biological implications involves two condensed phases: a liquid phase, L, and a condensed phase, LC. This phase transition corresponds to a conformational change where one α-helix segment of approximately 28.5 Å desorbs from the subphase leaving the other (40.5 Å) lying on the surface. Direct evidence of these conformational changes has been shown using grazing incidence X-ray diffraction and atomic force microscopy (AFM) scanning of Langmuir–Blodgett (LB) films of transferred monolayers.[3] Experiments on more complex interfaces have been prepared adsorbing APO CI on phospholipid (DPPC) monolayers, which indicate that apolipoproteins penetrate the DPPC monolayer to form part of the monolayer at the air–water interface.[7] These monolayers present two clear phase transitions between condensed phases, as well as one between a condensed phase and a gas phase. A model for understanding the phase transitions in these binary systems has been presented.[7]

When two surfaces with adsorbed layers of proteins are brought together, they will interact with each other. The resulting force versus distance curve will depend on the kind of surface, the solution conditions, and the type of protein. Therefore, the

* To whom correspondence should be addressed. E-mail: Jose.Campos@fkem1.lu.se. Current address: Physical Chemistry 1, University of Lund, P.O. Box 124, S-221 00 Lund, Sweden.

surface force apparatus (SFA)[8,9] offers the possibility of measuring the softness of the absorbed layers and the long-range and contact forces between adsorbed layers, as well as the absorbed layer thickness that helps in gaining information about the conformational structure and size of the adsorbed protein. The comparison between theoretical and experimental curves is not straightforward, since the measured force is the consequence of various force contributions that are interrelated and not strictly independent. The electrostatic double-layer force and the van der Waals force are considered the most important contributions, and even in these cases there are complications. The location of the plane of charge from which the double layer force acts is not well-defined, and the dielectric properties of the adsorbed protein layer are also not well-known. Globular proteins, like insulin and lysozyme, and proteins with unordered structure have been extensively studied with SFA techniques.[10]

The aim of this paper is to present our measurements for the interaction of adsorbed films of a protein mostly made of α-helices with an amphiphilic character, i.e., APO CI. Here, this protein has been adsorbed on hydrophilic and on hydrophobic substrates from a water solution. We used mica as a hydrophilic substrate, and as a hydrophobic substrate, we used covered mica obtained through LB deposition of octadecyltriethoxysilane (OTE). As we will show below, interaction forces between layers of APO CI adsorbed on hydrophilic and on hydrophobic surfaces are mainly composed of electrostatic double-layer forces at large surface distances and by steric repulsive forces at small distances.

Experimental Section

Reagents. Lyophilized human apolipoprotein (APO) CI (>98%, PerImmune Inc.) was used solubilized in water. The protein integrity was tested through far-UV circular dichroism.[2] Water was ultrapure Milli-Q water (Nanopure-UV; 18.3 MΩ), filtered through a 0.22 µm membrane filter prior to being injected into the SFA. Octadecyltriethoxysilane (OTE) (94%, Lancaster Synthesis Ltd.) was used without further purification. The spreading solutions were made with chloroform (99% HPLC grade, Aldrich). Glassware was cleaned with hot chromosulfuric acid and rinsed with large quantities of water. All experiments were carried out in a dust-free environment.

Surface Force Measurements. An interferometric SFA was used to assess the interaction between adsorbed layers of APO CI on hydrophilic (mica) and on hydrophobic surfaces (mica-OTE). The instrument and procedures have been described by Israelachvili,[8] and the particular version of the apparatus used in this study (Mark IV) has been described by Parker.[9] Force is measured between two curved mica surfaces (mean radius of curvature, R, of ∼1–2 cm) in a crossed cylinder configuration made with two mica sheets, supported on half-cylindrical silica disks, where the first one is mounted on a double-cantilever spring (with a spring constant K) and the second one on a piezoelectric crystal. The surface separation, d, between the two surfaces is controlled by the piezoelectric crystal, and it is measured using an interferometric technique (accuracy of 2 Å). The magnitude of the force, F, as a function of the surface separation and normalized with respect to the mean radius curvature, can be determined from the spring deflection measured down to ca. 10^{-7} N. The mica sheets were made of green muscovite mica (S&J Trading Inc.), which were cleaved into molecularly smooth thin sheets, cut into 1 cm × 1 cm pieces. These are placed on a freshly cleaved mica backing sheet, where a silver layer ∼520 Å in thickness was deposited through evaporation. The mica pieces were glued using an epoxy resin

(EPON 1004F, Shell Chemical Co.) with the silver side down onto the optically polished half-cylindrical silica disks, and finally mounted in the SFA. The instrument, equipped with a large volume chamber (400 mL), was dismantled, and all its inner parts were rinsed with water and ethanol and finally blown dry with ultrapure nitrogen before they were assembled again. The assembly of the instrument and surface preparation were performed in a clean room under essentially dust-free conditions. All force measurements were carried out at 21 °C.

Monolayers and Hydrophobic Covered Mica. Mica surfaces were made hydrophobic with a Langmuir–Blodgett deposit of OTE according to the procedure developed by Wood and Sharma[11,12] and Campos et al.[13] Approximately 60–70 µL of a chloroform solution of OTE (∼1 mg/mL) was spread onto an acidified water subphase (using HNO_3, pH 2) to form a monolayer with an area per molecule of >60 Å. After spreading the OTE solution, we waited for polymerization until the pressure drop was negligible; typical waiting times were ca. 15 min. The degree of monolayer polymerization was observed with Brewster angle microscopy (BAM). We compressed the film at a rate of 15 cm²/min, and LB was deposited on mica at a constant lateral pressure of 10–12 mN/m (T = 23 °C). Mica pieces, either small (∼1 cm²) and thin pieces already glued in the silica disks for the SFA, or relatively big (∼2 cm²) and thick ones for AFM, were previously activated by a radio frequency-generated air/H_2O plasma (∼2 min at ∼30 W and 100 mTorr) in a Harrick Plasma Cleaner (PDC-23G). After deposition, the hydrophobic mica surfaces were baked and annealed for *2* h in a vacuum oven (100 °C, 100 mTorr) before being used. All monolayers and LB films were prepared on a computerized Nima LB trough (TKB 2410A, Nima Technology Ltd.) using a Wilhelmy plate to measure the lateral pressure ($\Pi = \gamma_o - \gamma$), i.e., the surface tension difference between the clean subphase, γ_o, and the silane-covered subphase, γ. The temperature was kept constant at 23 °C with the aid of a water circulator bath (Cole-Parmer model 1268-24).

Surface Measurements on Hydrophilic Surfaces (Mica). Two different methods of protein adsorption were used on hydrophilic surfaces. For the first method, experiments began measuring the mica–mica contact position in air. After a drop of the APO CI (1 mg/mL) solution was deposited between the SFA surfaces, after ∼1 h the SFA chamber was filled with water to reduce the concentration between the surfaces. In the second method, after the mica–mica contact position had been measured, the chamber of the SFA was filled with water. The contact position and a force curve were then recorded to verify the system was clean. Afterward, a pre-established amount of APO CI was added into the SFA chamber to allow a slow protein adsorption from the solution surrounding the surfaces.

Surface Measurements on Hydrophobic Surfaces (Mica-OTE). The mica–mica position was measured with the SFA in air. If the contact was found to be adhesive and free of particles, OTE was LB deposited on the mica sheets glued to the silica disks. Then, the silica disks were mounted back in the SFA, and the thickness value of the deposited OTE monolayer was determined. The SFA chamber was filled with water with the apparatus turned with the side port up to be able to aspirate the air–liquid interface during the filling to make sure that the air–water interface passed the mica surfaces as clean and as quickly as possible. Water was degassed by boiling under vacuum for several hours before the SFA was filled. These procedures reduce the level of contamination and minimize the risk of air bubbles sticking on the hydrophobic surface. The contact position and a force curve were then recorded in water.
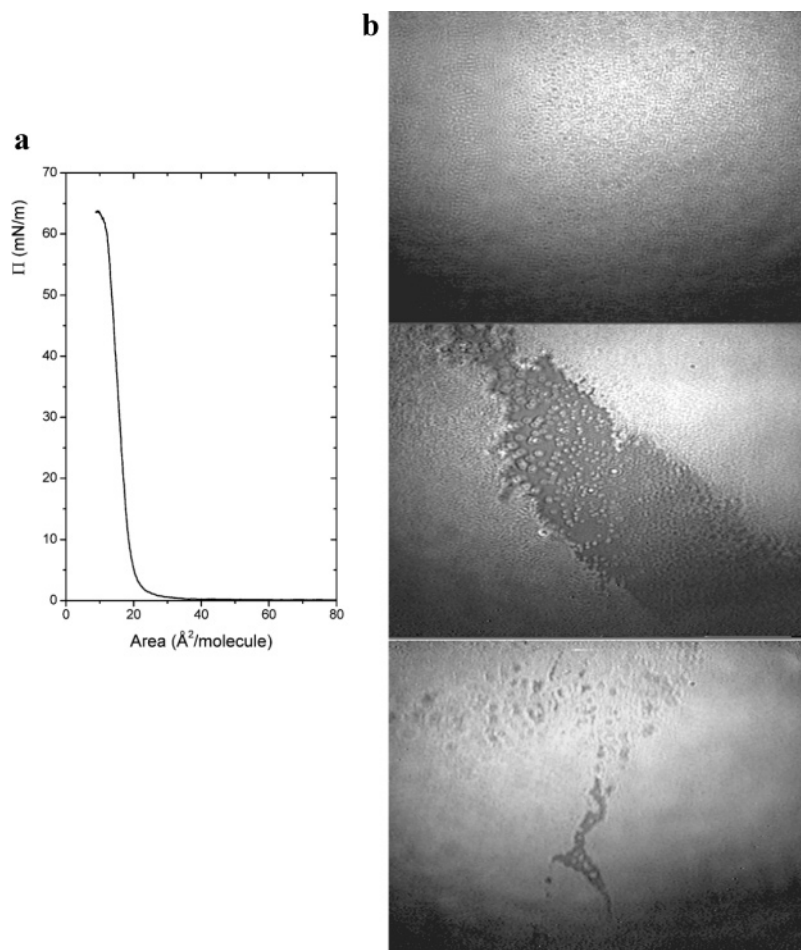
Figure 1. OTE monolayers at the water−air interface at 23 °C. (a) Typical isotherm for octadecyltriethoxysilane. (b) BAM images. Homogeneous coverage, in the top panel ($\Pi \sim 0$ and $a = 60$ Å^2/molecule). Imperfect coverage in the middle and bottom panels ($\Pi = 0$ mN/m and $a = 47$ Å^2/molecule, and $\Pi = 15$ mN/m, respectively). The horizontal breadth corresponds to 850 μm.

Only if the system was clean was an amount of APO CI added to the SFA chamber. The pH in all the SFA experiments was approximately 6.7. Taking into account this working pH and the calculated pK_a's for each amino acid in the APO CI protein, we find the net charge to be +1. No salt was added in any of the experiments.

Brewster Angle Microscopy. BAM observations were performed in a BAM1 Plus instrument (Nanofilm Technologie GmbH) with a spatial resolution of ca. 4 μm. Here, the interface is illuminated at the Brewster incidence ($\sim$53°) with a polarized laser beam from a He−Ne laser (632.8 nm). A microscope receives the reflected beam that is analyzed by a polarization analyzer, and the signal is received by a CCD video camera to develop an image of the monolayer.

AFM Observations. OTE LB-transferred monolayers on mica were scanned with two AFM instruments. A NanoScope IIIa SPM instrument (Digital Instruments) with a 15 μm × 15 μm scanner and a JSTM-4200 JEOL (JEOL) scanning probe microscope with a 10 μm × 10 μm scanner were used. Contact or intermittent contact modes were used to obtain topographic, deflection, and phase images.

Results and Discussion

OTE Films. In Figure 1a, we present a typical Π−a isotherm for an OTE monolayer deposited on an acidified water subphase that is essentially the same as that obtained by Wood and Sharma.[11] Hydrolysis and condensation polymerization take place very quickly, even before compression begins. This

monolayer was used to cover the mica surfaces through LB deposition. As far as we know, there are no previous reports of direct observations of this monolayer. In Figure 1b, we observe the OTE film as a finely woven net along the entire field of view at a vanishing lateral pressure ($a = 60$ Å^2/molecule). This net presents very small holes, which become even smaller as the lateral pressure is increased. Here, the film seems to be composed of large homogeneous domains ($\Pi > 10$ mN/m) at the BAM resolution, with a size on the order of millimeters with a few scattered holes. The surface pressure in the isotherm only begins to rise when these domains are forced to be together ($a \leq 25$ Å^2/molecule). However, the monolayer can also present extended areas where the flat polymerized domains do not cover homogeneously the air−water interface when $\Pi > 0$ mN/m (Figure 1b). This is a problem in obtaining homogeneous LB transferences. The defective areas are usually formed at very early stages of polymerization due to the formation of macroscopic irregular polymerized domains and to the rigidity of the polymerized monolayer net. When the monolayer is compressed, most of the big domains seem to heal at the BAM resolution. However, in some cases, defective areas remain upon compression, despite the fact that the isotherm does not show any appreciable changes (Figure 1b). These areas that are not well-covered look like the usual gas-condensed phase coexistence in Langmuir films when observed with a BAM. More homogeneous films were obtained when dilute spreading solutions (<1.2 mg/L) were used in combination with a careful and a
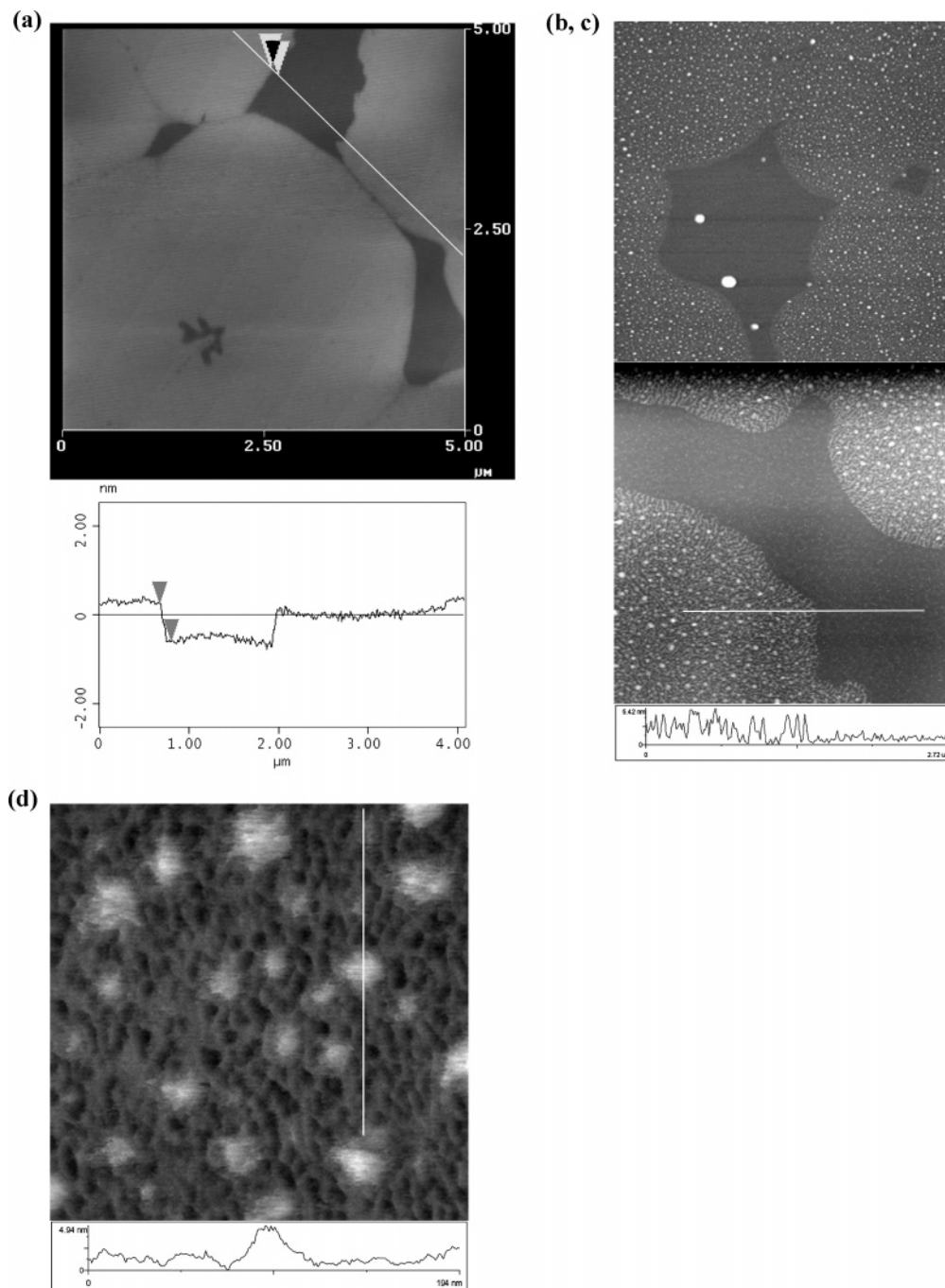
α-Helical Human Apolipoprotein CI

J. Phys. Chem. B, Vol. 108, No. 52, 2004 **20445**

Figure 2. AFM images of OTE films over mica. (a) OTE 5 × 5 μm image of OTE film transferred at 12 mN/m without important defects and revealing island domains (contact mode). Intermittent contact mode images: (b) 5 × 5 μm image of OTE film transferred at 12 mN/m, where the prepolimerized OTE was exposed to water traces; (c) 6 × 6 μm image of the OTE film similar to that presented in panel b, except that the spreading solution was filtered (transference at 12 mN/m) (condensed and gas phase domains formed in the monolayer prior to the transference are clearly observed); and (d) 250 × 250 nm image of the protruding aggregates over the condensed phase presented in panel b.

homogeneous dropping of the spreading solution along the trough.

When AFM was employed, as shown in Figure 2a (contact mode), big round and flat domains in the LB-transferred OTE monolayers (at ca. Π = 12 mN/m) were observed, very similar to those reported by Wood and Sharma.[12] BAM and AFM images support the general belief[11,13] that when the OTE film is spread on the air−water interface at relatively large molecular areas ($a > 25$ Å^2/molecule), the film is composed of isolated polymerized islands, similar to a condensed phase surrounded by a gas phase, as in gas-condensed phase transitions seen in conventional amphiphiles. The condensed domains and the gas phase must be in thermal as well as chemical equilibrium

because of the polymerization reaction. With AFM, we found that on average the height difference between the condensed phase round domains and the gas phase domains in the transferred films is 1.2 ± 0.4 nm. On the other hand, the average film thickness is ca. 2.4 nm measured with the SFA (between mica-covered surfaces at contact); this value agrees with the previously reported value of 2.1 nm.[13]

The baking procedure after the LB transfer of the OTE monolayer is expected to iron out possible strained configurations between the condensed domain boundaries and, also, to stitch individual islands together across the domain boundaries by completing the in-plane polymerization.[11] Additionally, the heating is also expected to remove the vicinal water sandwiched

between the OTE silanol groups and the mica surface, thereby creating a stable monolayer.[11,14] Also, it is believed that a small amount of covalent attachment does occur between the ethoxysilane with the plasma-treated mica surface when baked at 100 °C.[11,14] All these factors produce a stable and robust hydrophobic OTE monolayer.

From the discussion of BAM images given above, an important comment must be made here since it is easy to conclude that the higher the transference pressure that is used, the better LB film is obtained; i.e., fewer defects are left by the monolayer. However, AFM scanning of samples transferred above lateral pressures of ∼15 mN/m reveals that some material is sent out from the monolayer forming three-dimensional (3D) protruding aggregates (small white blobs) upon the monolayer (their diameter is on the order of 50−100 nm, and their heights can reach up to ∼7 nm). These 3D aggregates can be seen in the AFM images presented in Figure 2b−d. Similar aggregates have been observed in self-assembled monolayers of OTE[15] and in the LB deposit of heptadecafluorotetrahydrodecyltriethoxysilane on molten glass.[16] They were explained as a product of 3D polymerization in the prehydrolysis solution. These 3D protruding aggregates cannot be detected with BAM because of the low contrast of the monolayer and the limited BAM spatial resolution (<4 μm). However, sometimes it is possible to see localized oscillations[17] and buckling[18] in the monolayer, considered mechanisms of expulsion of material from the monolayer in rigid monolayers, below the collapse. The 3D protruding aggregates are scarcely found when the prepolymerized OTE is handled with extreme care and when transferences are made at lateral pressures Π of ∼10−12 mN/m. In particular, contact with traces of water when preparing the chloroform spreading solution must be avoided, since it produces tiny polymerized clusters. Figure 2b shows an AFM image of a transferred OTE film at 12 mN/m, with protruding aggregates (small bright spots) where the prepolymerized OTE was exposed to water traces. Filtering the prepolymerized solution through 0.020 μm filters prior to dropping helps to lower the number of 3D aggregates; nevertheless, we could not eliminate them all (see Figure 2c). Here, the condensed and gas phase domains of the polymer film are quite clear, confirming that in the gas phase domains there is also coverage, although less dense than in the condensed domains. AFM images of the gas phase at larger amplification (not shown) present very small and scattered protruding aggregates. Figure 2d shows an OTE film AFM image of the condensed phase with the protruding aggregates. These aggregates are not very well defined because of their floppy nature, when sensed with the AFM tip.

Surface Force Interaction. *Proteins Deposited on Hydrophilic Surfaces.* Figure 3 shows two force curves measured consecutively after deposition of a small drop (0.1−0.2 mL) of an APO CI solution directly over the mica surfaces and after dilution of this solution when the SFA chamber (≈400 mL) is filled with water. Prior to the force measurements, the surfaces were left to equilibrate for more than 24 h separated at 2 mm. On the first approach, almost no forces were measured until *d* approached ∼200 Å (*d* is the surface separation), where a repulsive steric force with a clear in−out movement of the surfaces was found; i.e., the surfaces moved closer and apart spontaneously between the times for each measurement. The range of movement is ∼60 Å centered at *d* ∼ 70 Å. As time elapses, the surfaces move slowly to an equilibrium *d* ∼ 45 Å. Here, if we try to bring the surfaces closer together, the surfaces separated and the in−out movement restarted. The last points in the force curve were measured without using the piezoelectric
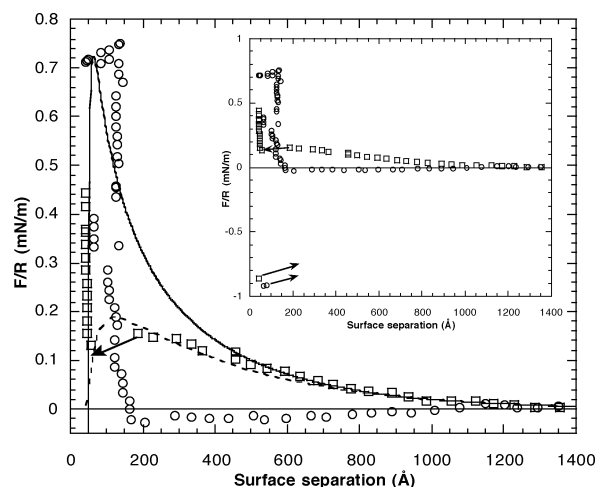

Figure 3. Force, *F* (normalized by the radius of curvature, *R*), as a function of surface separation measured consecutively for two mica surfaces where a direct deposit of APO CI was made and left to equilibrate for more than 24 h. Almost no forces were found in the first approach (○) until a repulsive steric wall was found around 150 Å of surface separation; as time elapsed, they approach a final equilibrium distance of 45 Å. On the second approach (□), an electrostatic repulsive force is found below 1200 Å until an attractive force around 185 Å moves the surfaces to a distance of 57 Å. Further compression takes the surfaces to a value of 40 Å. The solid line represents a DLVO fitting at a constant surface charge and the dashed line at constant surface potential. The inset shows the last point measured on each curve before the surfaces move apart, showing that there is some adhesion between the surfaces. Arrows show the directions of the attractive jump on approach and of adhesive jumps when surfaces are taken apart.

to approach the surfaces. A waiting time of 1−3 min was spent between each measured point. On a second consecutive approach, the force curve shows a long-range repulsive force. As the surfaces are brought closer together, the repulsive force is overcome by an attractive force at *d* ∼ 185 Å; this force brings the surfaces into contact at *d* = 57 Å. Further compression does not allow it to go beyond *d* ∼ 40 Å, suggesting that the adsorbed layer has a very low compressibility. The long-range repulsive force and the attractive force can be fitted using DLVO theory, including additive contributions of nonretarded van der Waals forces and the electrostatic double-layer force (see Figure 3). Calculations of double-layer force were performed with the algorithm of Chan et al.,[19] bringing into play both constant surface potential and constant surface charge. In practice, it is most likely that both potential and surface charge vary as the surfaces approach, where the actual double-layer force, as in our case, falls between these two limits because of charge regulation. To fit this curve, we put the plane of charge and the origin of the van der Waals forces at the onset of the steric wall (40 Å) and used a Hamaker constant of 0.5 × 10⁻²⁰ J, which is the value for a hydrocarbon layer interacting across water, as a common value used like a first guess for protein layers.[10] In this case, the fitting value for the surface potential is 40 mV, and the decay length is 320 Å, which corresponds to a 1:1 electrolyte concentration of 9 × 10⁻⁵ M. Note that although DLVO theory does not take into account additional forces occurring between the surfaces, e.g., hydration forces, hydrophobic forces, and steric forces, etc., the fitting is quite good, and the attractive force measured is close to what theory suggests, at a constant surface charge. In both measurements, we found an adhesive contact when separating the surfaces (see the inset in Figure 3) with a measured pull-off force of 5.6 mN/ m, indicating that there is some interaction between the adsorbed
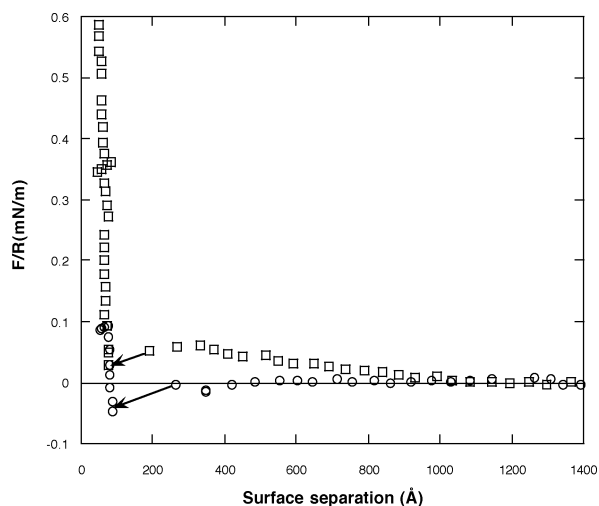
Figure 4. *F/R* as a function of surface separation measured consecutively between two mica surfaces where a direct deposit of APO CI was made, after dilution and equilibration for 32 h. The same cycle of forces was measured as in earlier times (see Figure 3), but an attractive force found in the first approach (○) that brought the surfaces from above *d* = 200 Å to *d* = 78 Å. Also, it is clear how the in−out movement exhibited at earlier approaches is reduced.

layers of APO CI. Directional adsorption of APOs prefers the hydrophilic faces of the protein α-helices to be adsorbed onto the mica, leaving the hydrophobic faces of the α-helices in contact with water. Therefore, the strong adhesive interaction is probably carried out between these hydrophobic faces, which try to avoid the exposure of the hydrophobic faces to water when surfaces are moving apart. APO CI has a high conformational stability, since we did not observe any changes in the surface separation when compressing the adsorbed protein layers (steric walls in the force curves) or when we took the surfaces apart. If the surfaces are left at surface separation ca. 3000−4000 Å for ∼8 h, the same cycle of forces was again measured, although in some measurements, we also observed an attractive jump in the first approach (see Figure 4). The same forces were found in other contact positions of the surfaces.

Because of the quantity and the way proteins were allowed to adsorb on the surfaces, and to the net positive charge (+1) of APO CI under the conditions of the experiment, it is not strange that the protein had neutralized the negative charge of the mica surface; a confirmation is the lack of force above *d* = 200 Å. A similar process has been observed in SFA studies with lysozyme.[20] Here, as in the case of lysozyme, a recharge of the surfaces with a sign different from the original one was not observed due to different causes. APO CI adsorbs through most of its positive charges to the negative mica surface, and in that way, the ionizable groups are transferred to a region with a low dielectric constant (hidden from the solution), producing a change in the acid−base equilibrium to an uncharged state. The adsorption is followed by an ionic exchange, where protons and ions that are in the solution are displaced from the mica surface.[21,22]

When the surfaces approach a distance near double the length of the long size of APO CI, ∼140 Å, on the first approach, proteins seem to almost make contact because they interact between them in a repulsive way. As we decrease the surface separation, the increase in the repulsive force suggests that APO CI proteins are forced to organize themselves in the space available between the surfaces. The in−out movement of the surfaces, as we take them further in, is an unusual behavior that is difficult to explain. One possible explanation to this

phenomenon is related to elastohydrodynamic lubrication.[23] It has been observed before that weakly adsorbed proteins tend to be squeezed out from the edges of the contact zone under pressure, but because of their relatively large size, they tend to be trapped in the middle of the contact zone.[24] In such cases, the interferometric fringes used to measure the surface separation will obtain a bell shape that makes distance determination difficult.[24] However, we did not see the bell-shaped fringes, so this explanation only fits to our case if we consider that this effect was possible at the low compressive forces applied, due to a combination of the amount of protein adsorbed on the surfaces and some special characteristic of APO CI conformation (two α-helices). The extent of this in−out movement was reduced in subsequent measurements (see Figure 4), most probably because the excess layers were permanently removed or because they self-organize in a different form.

The fitting of the repulsive force to DLVO theory confirms the electrostatic origin of the force, on the second approach. The charge of the surfaces can be explained if we consider that when we took apart the surfaces, after the first approach, we perturbed the adsorbed protein layers. This perturbation could remove some of the adsorbed proteins, exposing the charged groups and reducing the neutralization of the mica surfaces, with a consequent surface charge. Also, this perturbation could produce a surface configuration of the proteins where parts of them are dangling or protruding from the surfaces, which in consequence could produce the observed attractive force due to entanglement of the α-helices. Attractive forces due to protruding or extended parts of proteins have been observed before with protein A adsorbed on mica[25] and with β-casein adsorbed on a hydrophobic mica surface.[26] In addition, the final distance of 40 Å seems to corroborate that some part of the proteins could be adsorbed on the surface and another part could be protruding to the solution in the gap. This agrees with the model of the APO CI monolayer at interfaces proposed by us.[2,3] One thing to mention is that, although the fitting of our curves shows that the van der Waals interaction makes an important contribution to the attractive force found, we have to consider that the fitting was done considering the extreme case, i.e., a Hamaker constant for a hydrocarbon−water−hydrocarbon interaction, and we have to take into account that there might be some amount of water in the adsorbed protein layers which will reduce the Hamaker constant and the magnitude of the van der Waals interaction. Hence, it also is likely that other forces contribute to the attractive force, such as interactions due to hydrophobic patches and/or oppositely charged amino acid residues between the protruding α-helical segments of the proteins, as we are proposing.

Figure 5 shows force curves measured when APO CI was allowed to adsorb from the water solution surrounding the surfaces. Previously, the force curve between the curved surfaces in water was measured (inset of Figure 5). This curve is similar to the ones measured by others[27,28] and shows a long-range repulsion associated with the presence of charge on the mica surfaces, arising from the loss of potassium ions to the solution. A big change in the force curve was found when APO CI was injected into the SFA chamber, and it was allowed to adsorb for more than 12 h to give a final concentration of 1.5×10^{-8} M (pH ∼7). Here, no forces were found until *d* ∼ 1000 Å, where a very small repulsive force is observed. This repulsive force increases its magnitude, up to *d* ∼ 14 Å. A consecutive force curve was measured that presents characteristics similar to those of the first one. In both cases, a strong adhesive force (∼440 mN/m) was found when the surfaces were taken apart.
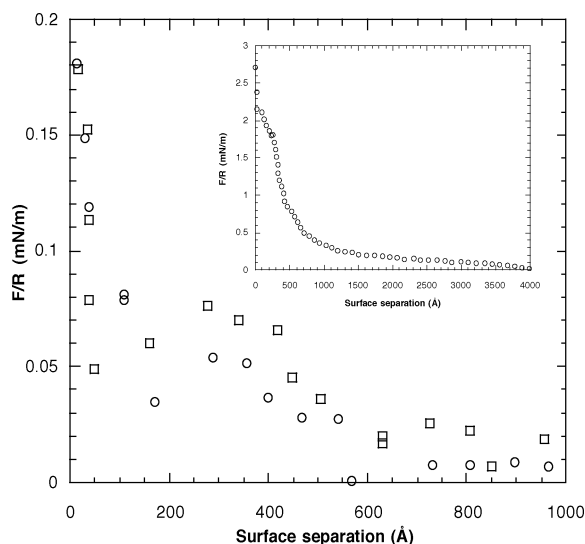
Figure 5. *F/R* as a function of surface separation for surfaces of mica coated with APO CI adsorbed from the water solution that surrounds the surfaces. Two consecutive measurements, (○) first and (□) second, were taken at the same contact position ~12 h after the injection of the protein. Both measurements present a small repulsive force below 1000 Å until a final surface separation of 14−16 Å was reached. Observe the very small magnitude of the forces measured. The inset shows the measured force curve between the same mica surfaces in water.

Figure 6. *F/R* as a function of surface separation for consecutive measurements more than 48 h after APO CI was injected into the SFA chamber. The force curve measured in the first approach (○) presents a repulsive force below 600 Å until an attractive force takes the surfaces from $d = 105$ Å to $d = 5$ Å. No forces were present in the second approach (○) until an attractive force takes the surfaces from $d = 131$ Å to $d = 24$ Å. The arrows are only guides to the eye to show the direction of the attractive jumps. The solid line and the dashed line represent the DLVO curves at a constant surface charge and a constant surface potential, respectively, using a surface potential of 15 mV and a decay length of 350 Å and assuming that the plane of charge is at a distance of 5 Å.

Here, the scattering of the points that were obtained is a result of the small magnitude of the force measured that is close to the force resolution of the SFA (0.005 mN/m). Since APO CI has a positive net (+1) charge under the conditions of the experiment, it will adsorb favorably on the negative mica, and probably more important, there is a large entropy increase upon liberation of counterions. The observed reduction in the long-range repulsive force confirms the screening effect produced by the presence of the charged protein between the surfaces, and the final distance values indicate that there is adsorption of APO CI, which results in a partial surface charge neutralization. However, the presence of a small repulsive force and the large adhesion found indicates that the protein does not completely cover the mica surface. From the final $d \approx 14−16$ Å, and taking into account that an α-helix is between 5 and 7 Å in diameter; we suspect that the protein is adsorbed side-on to the surfaces. The final layer thickness value of 7−8 Å for one surface is similar to the value observed at Langmuir−Blodgett-transferred monolayers of APO CI characterized with AFM.[3] The conformation of proteins whether in solution or adsorbed onto a solid substrate is determined by a delicate balance of intramolecular and intermolecular interactions. Nevertheless, although structure modification caused by the adsorption of the helices is expected here, it has been proved before[29] that these structural changes are not enough to completely disturb the α-helix structure, and the final thickness value that we found seems to corroborate this.

Figure 6 shows two force curves measured consecutively more than 48 h after APO CI was injected into the SFA chamber. We consider that at this point the adsorption process of APO CI has come to equilibrium. The force curve measured on the first approach is similar to those shown in Figure 5, but in this case, the long-range force shows a clear electrostatic double-layer force. We also observed a steric wall around 140 Å and an attractive force, which causes the protein-covered surfaces to slide into contact at $d = 5$ Å. The presence of a steric barrier here could have different explanations. One is that
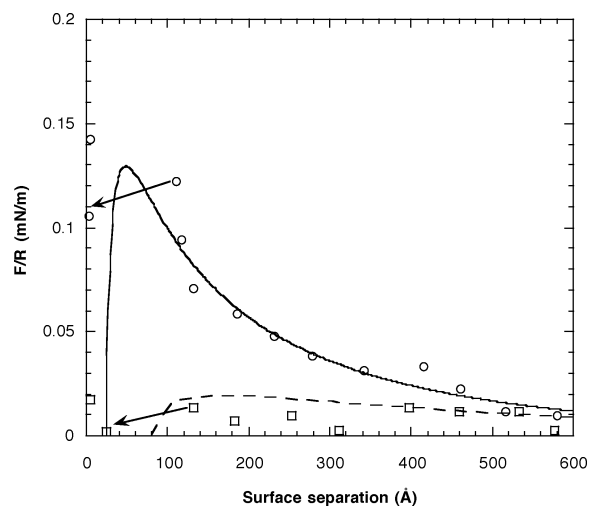
there are a few adsorbed layers of APO CI, which are removed from the contact area when the surfaces are brought together. The formation of multilayers is reasonable to avoid the possibility that the hydrophobic part of the protein could be exposed to the water solution. Another possibility could be that many of the adsorbed proteins have only one of their α-helices bound to the surfaces and the other one dangling into the solution. These protruding α-helices could interact with each other when the surfaces are brought closer, producing a repulsive force once the outer segments begin to overlap. This interaction usually leads to a repulsive osmotic force due to the unfavorable entropy associated, in this case, with the confining of α-helices between the surfaces. This conformation has been shown by this protein at interfaces.[2,3] As we mentioned before, these protruded segments could also explain the attractive force found afterward. We consider that there is intercalating (entanglement) between α-helices or bridging between the surfaces produced by some segments of the protein that are adsorbed to one of the surfaces that feel an electrostatic attractive force due to proteins dangling from the opposite surface. For the case of polyelectrolytes between two charged surfaces, it is enough to be close to, but not necessarily bonded to, both surfaces to produce attraction,[30] and this could be our case. This kind of attractive force has also been observed before on surfaces adsorbed with β-casein,[26] which is a flexible but not globular protein, and with protein A.[25] On the second approach, there is a complete change in the measured force curve. Here, we do not observe almost any force until an attractive force drives the surfaces from $d \sim 131$ Å to $d \sim 24$ Å. If we took the surfaces further in, the final d was 5 Å. The fact that we did not measure any force before the attractive jump suggests that with the first approach an improved adsorption or reorganization of the adsorbed protein was produced with a conformation that was able to almost screen the charge of the mica surfaces. In this approach, and in the previous one, an adhesive pull-off force of 38 mN/m was measured when separating the surfaces. This
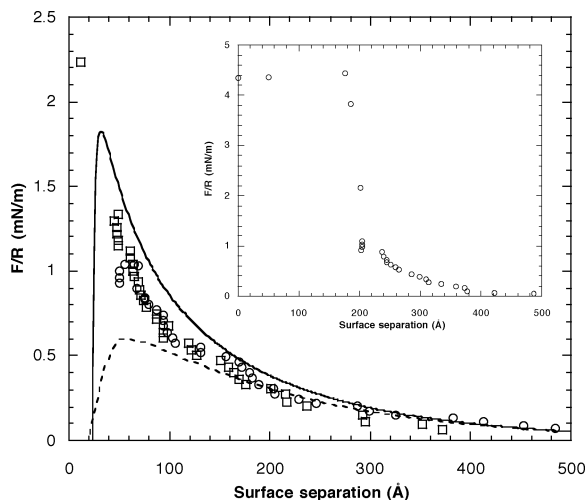
α-Helical Human Apolipoprotein CI

J. Phys. Chem. B, Vol. 108, No. 52, 2004 **20449**

Figure 7. *F/R* as a function of surface separation for hydrophobic mica surfaces, where APO CI was adsorbed from the water solution. The curves were measured 6 h (○) and 31 h (□) after APO CI was injected into the SFA chamber. Both curves present a long-range electrostatic double-layer repulsion, and the final distance separation changed from $d = 55$ Å to $d = 14$ Å. The solid line represents the DLVO fittings at a constant surface charge and the dashed line at a constant surface potential where the plane of charge was kept at 14 Å. The inset shows the force curve measured between OTE−mica surfaces in water.
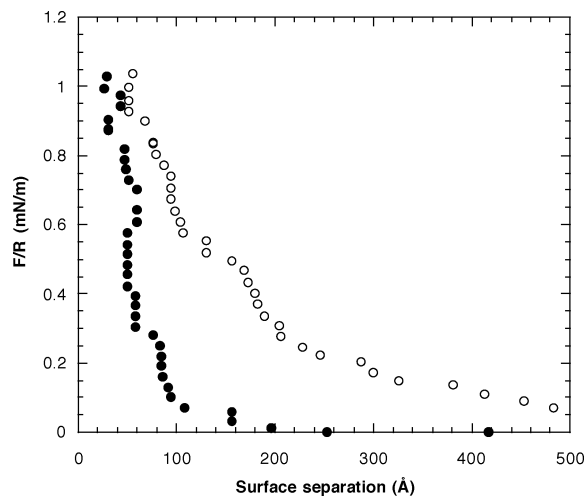

Figure 8. *F/R* as a function of surface separation measured on approach (○) and on separation (●) between two hydrophobic mica surfaces where APO CI was adsorbed from the water solution. Hysteresis found in the force curves shows that there is a small adhesion between the protein-adsorbed surfaces.

reduction in the extent of adhesion supports the idea of a larger adsorption or better coverage due to reorganization on the surfaces, compared to what we measured at earlier times of adsorption (∼440 mN/m).

One interesting point is the difference in the final thickness of the adsorbed protein layer when we compare it with the previous type of experiment (5 Å vs 40 Å). We believe that this difference is related to the smaller concentration used in this case (3 orders of magnitude lower), which allows a better spreading of the protein at the surface with a side-on conformation.

Proteins on Hydrophobic Mica Surfaces. The force curve between plain OTE surfaces in water was measured prior to the measurement of the adsorbed APO CI (inset of Figure 7). It is important to mention that replicas of hydrophobic mica surfaces made at the same time as those used for SFA measurements were surveyed via AFM, and only those of good quality were used, like those shown in Figure 2a. Our curve is similar to the ones reported by Campos et al.,[13] where a repulsive force was found presumably produced by nanobubbles. There, the repulsive force disappeared when monoolein, a lipid with a very low solubility in water, was allowed to adsorb on the surfaces. Nanobubbles have been reported with other hydrophobic surfaces similar to the ones used here.[31−38] Reviews on this subject have been recently presented.[39,40] Figure 7 shows two curves measured between hydrophobic OTE surfaces after APO CI was adsorbed on. The curves were measured 6 and 31 h after injection of the protein into the SFA chamber to give a final concentration of 3×10^{-8} M. The presence of APO CI eliminates the strong repulsive force found between the OTE surfaces in water. The adsorption of APO CI, as in the case of monoolein,[13] seems to reduce the solid−liquid interfacial tension facilitating the wetting of the hydrophobic surface by water; any bubbles on the surface will be destabilized. The zero surface separation for these force curves is defined as the contact value between OTE-covered surfaces, ca. 48 Å relative to the mica−mica contact. The measured curves present a long-range repulsive force, most probably of electrostatic origin. The surfaces can be approached until $d \sim 55$ Å, where further

compression does not significantly change the surface separation. Hysteresis in the *F/R* versus *d* curve (see Figure 8) shows that the contact is lightly adhesive, and the fact that there is not a large increase in the surface separation before the surfaces move apart indicates that the adsorbed layers have a marginal compressibility. The experimental curve measured after adsorption for 31 h is essentially the same as the one described before, but here the final *d* is 14 Å, suggesting that the proteins are adsorbed with a side-on conformation. If we use this surface separation as the onset of the plane of charge and the origin of the van der Waals forces, then the curves can be fitted by DLVO theory using a Hamaker constant of 0.5×10^{-20} J. The fitting gives a surface potential of 50 mV and a Debye length of 155 Å, which corresponds to a 1:1 electrolyte solution of 3.9×10^{-4} M.

Adsorption on a hydrophobic surface was expected here due to the amphiphilic character of APO CI, and in general, it is known that proteins adsorb to a larger extent on hydrophobic surfaces[10] instead of on hydrophilic surfaces. Also, the higher affinity of amphipatic α-helices for hydrophobic interfaces has been shown recently by interfacial tension measurements using a consensus sequence peptide.[41] This is the case for APO CI, since just 6 h after the injection of the protein we found a larger adsorption on the surfaces compared to the case of hydrophilic surfaces. From the lower value of adhesion that was found, compared with the adhesion between OTE surfaces (∼300 mN/m) and with the case of adsorbed APO CI on hydrophilic surfaces, we estimate a complete coverage of the hydrophobic surfaces by the protein. The electrostatic curves that were found seem to indicate that proteins adsorb with their hydrophobic side to the surface (hiding it from the water) and leaving the charged residues exposed to the water solution. The charged residues of adsorbed proteins, proteins between the surfaces, and counterions form an electrostatic double layer that is observed as a clear repulsive force. The reduction of the adsorbed layer thickness between the measurements is a result of the elimination of the outer layers adsorbed on the surfaces, and the small adhesion found between the layers seems to indicate that the side-on conformation adapted in this case by the proteins does not favor the interaction between them. Also, we do not observe any bridging or intercalating of the surfaces, as we saw in the case of hydrophilic surfaces. This is to be expected since bridging is only possible when there is a small

coverage of the surfaces which does not seem to be the case here. In general, since the interaction between hydrophobic surfaces and proteins is stronger, it seems to be more difficult that some of the α-helix segments of APO CI desorb to produce intercalating.

Conclusions

Interaction forces between layers of APO CI adsorbed on hydrophilic (mica) and on hydrophobic (OTE-mica) surfaces are mainly composed of electrostatic double-layer forces at large surface distances and by steric repulsive forces at small distances. In some cases, no forces were measured before a steric wall was found, suggesting that a complete neutralization of the surface charge was achieved by the protein adsorption. The protein layer thickness values that were found allow us to give an image of the organization and conformation of the APO CI proteins on the surfaces. We found that APO CI adsorbs on both hydrophilic and hydrophobic surfaces, but it is more favored at hydrophobic surfaces where the adsorption time was clearly shorter and a larger layer thickness was measured. The adhesion obtained in both types of surfaces indicates that the interaction between the hydrophobic sides of the APO CI proteins is stronger than the one produced by the hydrophilic side of the protein.

Of particular interest is the observed bridging or intercalating between APO CI layers on hydrophilic surfaces, because this could have implications on the way APO CI moves between lipoproteins. Also, it is important to mention that the magnitudes of the forces measured are, in some cases, unusually small and that can be an important factor during the exchange of APO CI between lipoproteins.

References and Notes

(1) Bolaños-Garcia, V. M.; Soriano-Garcia, M.; Mas-Oliva, J. *Mol. Cell. Biochem.* **1997**, *175*, 1.

(2) Bolaños-Garcia, V. M.; Mas-Oliva, J.; Ramos, S.; Castillo, R. *J. Phys. Chem. B* **1999**, *103*, 6236.

(3) Ruiz-Garcia, J.; Moreno, A.; Brezesinski, G.; Möhwald, H.; Mas-Oliva, J.; Castillo, R. *J. Phys. Chem. B* **2003**, *107*, 11117.

(4) Despres, J. P.; Lemieux, I.; Dagenais, G. R.; Cantin, B.; Lamarche, B. *Atherosclerosis* **2000**, *153*, 263.

(5) Bolaños-Garcia, V. M.; Ramos, S.; Castillo, R.; Xicohtencatl-Cortes J.; Mas-Oliva, J. *J. Phys. Chem. B* **2001**, *105*, 5757.

(6) Borhani, D. W.; Rogers, D. P.; Engler, J. A.; Brouillette, C. G. *Proc. Natl. Acad. Sci. U.S.A.* **1997**, *94*, 12291.

(7) Xicohtencatl-Cortes, J.; Mas-Oliva, J.; Castillo, R. *J. Phys. Chem. B*, in press.

(8) Israelachvili, J. N.; Adams, G. E. *J. Chem. Soc., Faraday Trans. 1* **1978**, *74*, 975.

(9) Parker, J. L.; Christenson, H. K.; Ninham, B. W. *Rev. Sci. Instrum.* **1989**, *60*, 3135.

(10) Claesson, P. M.; Blomberg, E.; Fröberg, J. C.; Nylander, T.; Arnebrant, T. *Adv. Colloid Interface Sci.* **1995**, *57*, 161.

(11) Wood, J.; Sharma, R. *Langmuir* **1994**, *10*, 2307.

(12) Wood, J.; Sharma, R. *Langmuir* **1995**, *11*, 4797.

(13) Campos, J.; Eskilsson, K.; Nylander, T.; Svendsen, A. *Colloids Surf., B* **2002**, *26*, 172.

(14) Kim, S.; Christenson, H. K.; Curry, J. E. *Langmuir* **2002**, *18*, 2125.

(15) Xiao, X. D.; Liu, G.; Charych, D.; Salmeron, M. *Langmuir* **1995**, *11*, 1600.

(16) Ohnishi, S.; Ishida, T.; Yaminsky, V. V.; Christenson, H. K. *Langmuir* **2000**, *16*, 2722.

(17) Galvan-Miyoshi, J.; Ramos, S.; Ruiz-García, J.; Castillo, R. *J. Chem. Phys.* **2001**, *115*, 8178.

(18) Bourdieu, L.; Daillant, J.; Chatenay, D.; Braslau, A.; Colson, D. *Phys. Rev. Lett.* **1994**, *72*, 1502.

(19) Chan, D. Y. C.; Pashley, R. M.; White, L. R. *J. Colloid Interface Sci.* **1980**, *77*, 283.

(20) Blomberg, E.; Claesson, P. M.; Fröberg, J. C.; Tilton, R. D. *Langmuir* **1994**, *10*, 2325.

(21) Herder, P. C.; Claesson, P. M.; Blom, C. E. *J. Colloid Interface Sci.* **1987**, *119*, 155.

(22) Rutland, M.; Waltermo, Å.; Claesson, P. M. *Langmuir* **1992**, *8*, 176.

(23) Roberts, A. D.; Tabor, D. *Proc. R. Soc. London, Ser. A* **1971**, *323*, 323.

(24) Blomberg, E.; Claesson, P. M.; Christenson, H. K. *J. Colloid Interface Sci.* **1990**, *138*, 291.

(25) Ohnishi, S.; Murata, M.; Hato, M. *Biophys. J.* **1998**, *74*, 455.

(26) Nylander, T.; Wahlgren, N. M. *Langmuir* **1997**, *13*, 6219.

(27) Raviv, U.; Laurat, P.; Klein, J. *Nature* **2001**, *413*, 51.

(28) Pashley, R. M. *J. Colloid Interface Sci.* **1981**, *80*, 153.

(29) Burkett, S. L.; Read, M. J. *Langmuir* **2001**, *17*, 5059.

(30) Åkesson, T.; Woodward, C. E.; Jönsson, B. *J. Chem. Phys.* **1989**, *91*, 2461.

(31) Attard, P. *Langmuir* **1996**, *12*, 1693.

(32) Attard, P. *Langmuir* **2000**, *16*, 4455.

(33) Christenson, H. K.; Claesson, P. M. *Science* **1988**, *239*, 390.

(34) Claesson, P. M.; Christenson, H. K. *J. Phys. Chem.* **1988**, *92*, 1650.

(35) Carambassis, A.; Jonker, L. C.; Attard, P.; Rutland, M. W. *Phys. Rev. Lett.* **1998**, *80*, 5357.

(36) Ishida, N.; Sakamoto, M.; Miyahara, M.; Higashitani, K. *Langmuir* **2000**, *16*, 5681.

(37) Ishida, N.; Inoue, T.; Miyahara, M.; Higashitani, K. *Langmuir* **2000**, *16*, 6377.

(38) Tyrell, J. W. G.; Attard, P. *Phys. Rev. Lett.* **2001**, *87*, 176104.

(39) Christenson, H. K.; Claesson, P. M. *Adv. Colloid Interface Sci.* **2001**, *91*, 391.

(40) Yaminsky, V.; Ohnishi, S.; Ninham, B. In *Handbook of surfaces and interfaces of materials*; Nalwa, H. S., Ed.; Academic Press: New York, 2001; p 131.

(41) Wang, L.; Atkinson, D.; Small, D. M. *J. Biol. Chem.* **2003**, *278*, 37480.